

HERMANN EMIL FISCHER (1852–1919) was considered by his father as too stupid to be a businessman and better suited to being a student, but he became the greatest chemist of his age. In addition to his lock-and-key model of enzyme specificity, he made major contributions to organic chemistry, including work on carbohydrates (especially their stereochemistry), purines, amino acids (he was the discoverer of valine and proline), proteins and triacylglycerols. In 1902 he became the second winner of the Nobel Prize for Chemistry, “in recognition of his synthetic work in the sugar and purine groups”. He was in poor health at the end of his life, caused in part by toxic effects of the heavy use of phenylhydrazine in his synthetic work, and after losing two of his sons in the First World War he committed suicide in 1919.

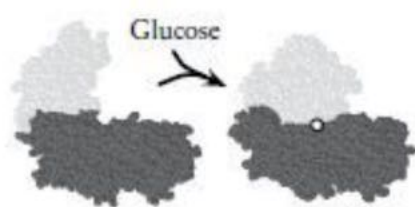


Figure 12.30. Conformational change of hexokinase D induced by binding of glucose. In the absence of glucose the two domains represented by the two degrees of shading are wide open, closing completely when glucose binds at a site behind the white circle.

12.4.2 Induced fit today

Now that the three-dimensional structures of many enzymes are known, not only in crystals but in solution in different states of the catalytic process, it has become clear that conformational changes induced by substrate binding are as general a phenomenon as Koshland envisaged. In enzyme mechanisms they range from changes so slight that they are barely observable to changes as large that induced by binding of glucose to hexokinase D, an enzyme discussed at the end of this chapter ([Section 12.9](#)) in the context of cooperativity in monomeric enzymes. This is illustrated in [Figure 12.30](#).

Even larger changes in conformation are found in *intrinsically unstructured proteins*. These are not enzymes, but are small proteins that only acquire a definite three-dimensional structure when bound to other proteins; otherwise they are random coils. For example, CP12 is a 9 kDa protein that

modulates the activity of the Calvin cycle in photosynthetic organisms by acting as a scaffold element in the formation of a supramolecular complex with glyceraldehyde-3-phosphate dehydrogenase and phosphoribulokinase. As Eralles and coworkers have shown, it is “chaperone-like”, which means that when bound to glyceraldehyde 3-phosphate dehydrogenase it protects the enzyme from aggregation and loss of activity.

12.5 The symmetry model of Monod, Wyman and Changeux

12.5.1 Basic postulates of the symmetry model

Cooperative interactions in hemoglobin are not unique in requiring interactions between sites that are widely separated in space; the same is true of other cooperative proteins, and of allosteric effects in many enzymes. A striking example is provided by the allosteric inhibition of phosphoribosyl-ATP pyrophosphorylase by histidine: Martin found that mild treatment of this enzyme by Hg^{2+} ions destroyed the sensitivity of the catalytic activity to histidine, but affected neither the uninhibited activity nor the binding of histidine. In other words, the metal ion interfered with neither the catalytic site nor the allosteric site, but with the connection between them. Monod, Changeux and Jacob studied many examples of cooperative and allosteric phenomena, and concluded that they were closely related and that conformational flexibility probably accounted for both. Subsequently, Monod and coworkers proposed a general model to explain both phenomena within a simple set of postulates. It has sometimes been called the *allosteric model*, but the term *symmetry model* emphasizes the principal difference between it and alternative models, and avoids the contentious association between allosteric and cooperative effects.

§ 12.9, pages 320–323

The symmetry model starts from the observation that each molecule of a typical cooperative protein contains several subunits. Indeed, this must be so for binding cooperativity at equilibrium, though it is not required in kinetic cooperativity ([Section 12.9](#)). The symmetry model for four subunits is shown in [Figure 12.31](#), but for simplicity I shall analyze the

symmetry model in terms of a protein with two subunits ($n = 2$), mentioning results for an unspecified number of subunits wherever those for $n = 2$ fail to express the general case adequately. Any number of subunits greater than one is possible, and any other kind of ligand (inhibitor or activator) can be considered instead of a substrate.

The symmetry model is based on the following postulates:

1. Each subunit can exist in two different conformations, R and T. These designations, nowadays regarded just as labels, originally stood for *relaxed* and *tense*, because the protein needs to relax to bind substrate, breaking some of the interactions that maintain its native structure in order to make new ones with the substrate.
2. All subunits of a molecule must be in the same conformation at any time; hence, for a dimeric protein, the conformational states R_2 and T_2 are the only ones permitted, the mixed conformation RT being forbidden. This condition is much more restrictive for more than two subunits. For example, for $n = 4$ the allowed states are R_4 and T_4 , and R_3T , R_2T_2 and RT_3 are all forbidden.
3. The two states of the protein are in equilibrium, with an equilibrium constant $L = [T_2]/[R_2]$.
4. A ligand can bind to a subunit in either conformation, but the intrinsic dissociation constants¹⁶ are different: $K_R = [R][A]/[RA]$ for each R subunit, $K_T = [T][A]/[TA]$ for each T subunit. The ratio K_R/K_T is sometimes written as c , but here we shall use the more explicit form.

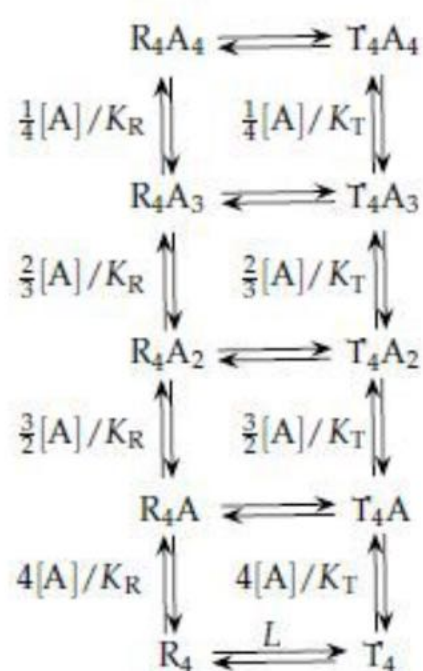


Figure 12.31. The symmetry model of Monod, Wyman and Changeux, illustrated here for a protein with four binding

sites. For analyzing the algebra in the text the simpler two-site model shown in [Figure 12.32](#) will be used.

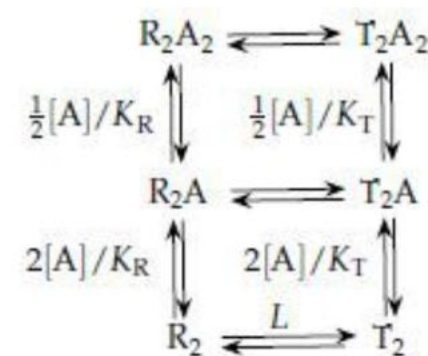


Figure 12.32. The symmetry model of Monod, Wyman and Changeux, illustrated here for a protein with two binding sites.

JEFFRIES WYMAN (1901–1995) was the third of the same name: his grandfather was a distinguished anatomist, and his father was an officer in the Bell Telephone Company. During his long career he made many contributions to protein chemistry, especially in relation to thermodynamics, and is particularly associated with the idea of *linkage* between different ligands that bind to the same protein—specifically to hemoglobin. He had met Jacques Monod while working in Paris between 1952 and 1955, and his famous paper with him and Changeux grew out of ideas that he had had much earlier. He spent much of his working life in Europe, in Cambridge, Paris, and especially Rome, where he remained for 25 years as a “temporary” guest scientist. He was active in a number of administrative roles, most particularly the establishment of the European Molecular Biology Organization (EMBO).

JEAN-PIERRE CHANGEUX (1936–) pursued his doctoral studies at the Pasteur Institute in Paris, under the direction of Jacques Monod and François Jacob, and during this time he worked on the theory of cooperativity. Subsequently he became one of the leaders in a different field, that of neurochemistry, and in that context he was the first to isolate a membrane pharmacological receptor, the nicotinic acetylcholine receptor of the eel electric organ.

12.5.2 Algebraic analysis

These postulates imply the set of equilibria between the various states shown in [Figure 12.32](#), and the concentrations of the six forms of the protein are related by the following expressions:

$$[R_2A] = 2[R_2][A]/K_R \quad (12.11)$$

$$[R_2A_2] = \frac{1}{2}[R_2A][A]/K_R = [R_2][A]^2/K_R^2 \quad (12.12)$$

$$[T_2] = L[R_2] \quad (12.13)$$

$$[T_2A] = 2[T_2][A]/K_T = 2L[R_2][A]/K_T \quad (12.14)$$

$$[T_2A_2] = \frac{1}{2}[T_2A][A]/K_T = L[R_2][A]^2/K_T^2 \quad (12.15)$$

In each equation, the “statistical” factor $2, \frac{1}{2}$ or 1 results from the definition of the intrinsic dissociation constants K_R and K_T in terms of individual sites although the expressions are written for complete molecules (compare [Section 12.2.5](#)). For example, $K_R = [R][A]/[RA] = 2[R_2][A]/[R_2A]$, because there are two vacant sites in each R_2 molecule and one occupied site in each R_2A molecule. The fractional saturation y is defined as before ([Section 12.2.5](#)) as the fraction of sites occupied by ligand, and takes the following form:

$$y = \frac{[R_2A] + 2[R_2A_2] + [T_2A] + 2[T_2A_2]}{2([R_2] + [R_2A] + [R_2A_2] + [T_2] + [T_2A] + [T_2A_2])}$$

In the numerator the concentration of each molecule is counted according to the number of occupied sites it contains (and so empty molecules are not counted at all), but in the denominator each molecule is counted according to how many sites it contains, whether occupied or not, and so each concentration is multiplied by the same factor 2. Substituting the concentrations from [equations 12.11–12.15](#), this becomes

$$y = \frac{\frac{[A]}{K_R} + \frac{[A]^2}{K_R^2} + \frac{L[A]}{K_T} + \frac{L[A]^2}{K_T^2}}{1 + \frac{[A]}{K_R} + \frac{[A]^2}{K_R^2} + L + \frac{2L[A]}{K_T} + \frac{L[A]^2}{K_T^2}} \quad (12.16)$$

$$= \frac{\left(1 + \frac{[A]}{K_R}\right) \frac{[A]}{K_R} + L \left(1 + \frac{[A]}{K_T}\right) \frac{[A]}{K_T}}{\left(1 + \frac{[A]}{K_R}\right)^2 + L \left(1 + \frac{[A]}{K_T}\right)^2}$$

Generalizing this for more than two subunits, the corresponding equation for n unspecified is as follows:

$$y = \frac{\left(1 + \frac{[A]}{K_R}\right)^{n-1} \frac{[A]}{K_R} + L \left(1 + \frac{[A]}{K_T}\right)^{n-1} \frac{[A]}{K_T}}{\left(1 + \frac{[A]}{K_R}\right)^n + L \left(1 + \frac{[A]}{K_T}\right)^n} \quad (12.17)$$

Monod, Wyman and Changeux wrote this equation in a superficially simpler form by replacing $[A]/K_R$ by α and $[A]/K_T$ by $c\alpha$:

$$y = \frac{(1 + \alpha)^{n-1} \alpha + L (1 + c\alpha)^{n-1} c\alpha}{(1 + \alpha)^n + L (1 + c\alpha)^n}$$

However, this just conceals the structure of the equation without changing anything fundamental.

12.5.3 Properties implied by the binding equation

The shape of the saturation curve defined by [equation 12.17](#) depends on the values of n , L and K_R/K_T , as may be illustrated by assigning some extreme values to these constants.

Special case 1. If $n = 1$, with only one binding site per molecule, the equation simplifies to

$$y = \frac{\frac{[A]}{K_R} + L \frac{[A]}{K_T}}{\left(1 + \frac{[A]}{K_R}\right) + L \left(1 + \frac{[A]}{K_T}\right)} = \frac{[A] \left(\frac{1}{K_R} + \frac{L}{K_T}\right)}{1 + L + [A] \left(\frac{1}{K_R} + \frac{L}{K_T}\right)}$$

This is much less complicated than it looks, because it can be written just as

$$y = \frac{[A]}{K_{RT} + [A]}, \text{ with } K_{RT} = \frac{1 + L}{\frac{1}{K_R} + \frac{L}{K_T}}$$

Despite the complicated expression for this dissociation constant, however, it is still a constant, and so the equation just defines a noncooperative binding function. In other words no cooperativity is possible if $n = 1$.

Special case 2. If $L = 0$, the T form of the protein does not exist under any conditions, and the factor $(1 + [A]/K_R)^{n-1}$ cancels between the numerator and denominator, leaving

$$y = \frac{[A]}{K_R + [A]}$$

This again predicts hyperbolic (noncooperative) binding.

Special case 3. A similar simplification occurs if L approaches infinity, and then the R form does not exist: in this case,

$$y = \frac{[A]}{K_T + [A]}$$

Special case 4. It follows from the first three examples that both R and T forms are needed if cooperativity is to be possible. Moreover, the two forms must be functionally different from one another, so that $K_R \neq K_T$. If $K_R = K_T$ it is again possible to cancel the common factor $(1 + [A]/K_R)^{n-1}$, leaving a hyperbolic expression. This illustrates the reasonable expectation that if the ligand binds equally well to the two states of the protein, the relative proportions in which they exist are irrelevant to the binding behavior.

General case. Apart from these special cases, [equation 12.17](#) predicts positive cooperativity, as may be seen by multiplying out the factors $(1 + [A]/K_R)^{n-1}$ and $(1 + [A]/K_T)^{n-1}$, and rearranging the result into the form of the Adair equation. For n sites the result is complicated, but the case for the dimer is adequately illustrative. [Equation 12.16](#) becomes

$$y = \frac{\left(\frac{1/K_R + L/K_T}{1+L}\right)[A] + \left(\frac{1/K_R^2 + L/K_T^2}{1+L}\right)[A]^2}{1 + 2\left(\frac{1/K_R + L/K_T}{1+L}\right)[A] + \left(\frac{1/K_R^2 + L/K_T^2}{1+L}\right)[A]^2} \quad (12.18)$$

Comparison of this with [equation 12.5](#) shows the two Adair constants to be as follows:

$$K_1 = \frac{1+L}{1/K_R + L/K_T}, \quad K_2 = \frac{1/K_R + L/K_T}{1/K_R^2 + L/K_T^2} \quad (12.19)$$

and their ratio is

$$\frac{K_2}{K_1} = \frac{(1/K_R + L/K_T)^2}{(1+L)(1/K_R^2 + L/K_T^2)} = \frac{\frac{1}{K_R^2} + \frac{2L}{K_R K_T} + \frac{L^2}{K_T^2}}{\frac{1}{K_R^2} + \frac{L}{K_R^2} + \frac{L}{K_T^2} + \frac{L^2}{K_T^2}}$$

As the outer terms in the multiplied-out numerator and denominator are the same, it is only necessary to examine the middle terms, and as $2xy$ is less than $x^2 + y^2$ for any values of x and y it follows that $K_1 > K_2$, so the model predicts positive cooperativity in terms of the Adair equation.¹⁷ Similar relationships apply between all pairs of Adair constants in the general case of unspecified n , and so the model predicts positive cooperativity at all stages in the binding process.

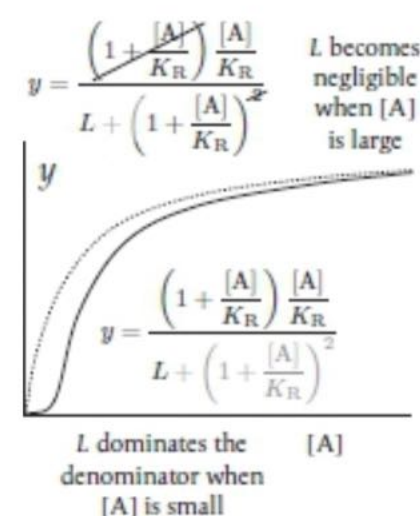


Figure 12.33. Explanation of [equation 12.20](#). When $[A]$ is small the denominator of the fraction is dominated by L , and the line remains close to the axis, but as $[A]$ increases L gradually becomes insignificant and the line approaches a rectangular hyperbola.

As this conclusion is algebraic rather than intuitive, it is helpful to examine one last special case, in which K_T is infinite and A binds *only* to the R state. This is a natural application of the idea of induced fit, though it is not an essential characteristic of the symmetry model as proposed by Monod, Wyman and Changeux. When K_T is infinite [equation 12.16](#) simplifies to

$$y = \frac{\left(1 + \frac{[A]}{K_R}\right) \frac{[A]}{K_R}}{L + \left(1 + \frac{[A]}{K_R}\right)^2} \quad (12.20)$$

Without the constant L in the denominator this would be an equation for hyperbolic binding, because the common factor $(1 + [A]/K_R)$ would cancel. When $[A]$ is sufficiently large L becomes negligible compared with the rest of the denominator, and the curve approaches a hyperbola. But when $[A]$ is small L dominates the denominator and causes y to remain initially very small as $[A]$ increases from zero. In other words, as long as L is significantly different from zero the curve of y against $[A]$ must be sigmoid.

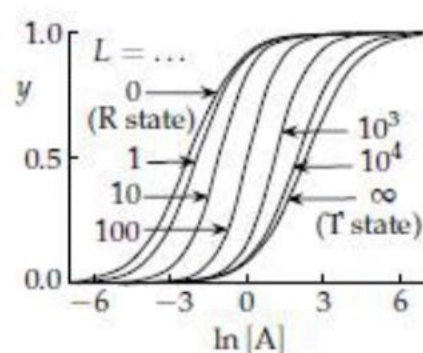


Figure 12.34. Binding curves for the symmetry model. The curves are calculated from [equation 12.18](#), with $K_T/K_R = 100$ and the values of L indicated.

When $K_R \neq K_T$, the degree of cooperativity, and hence the steepness of the curve, does not increase indefinitely as L increases, but passes through a maximum when $L^2 = K_T^2/K_R^2$. When this relationship is obeyed the half-saturation concentration ($K_{0.5}$ in [equation 12.1](#)) takes the simple form $K_{0.5} = (K_R K_T)^{0.5}$. However, as one may see from the representative binding curves calculated from [equation 12.16](#) shown in [Figure 12.34](#), this is in general an unreliable estimate; the best one can say in general is that the half-saturation concentration is between K_R and K_T . The figure was drawn with a logarithmic concentration scale. If it is redrawn with a linear scale ([Figure 12.35](#)) the differences between the different L values are much less obvious.

In the corresponding Scatchard plots ([Figure 12.36](#)) the extreme cases of $L = 0$ for the pure R state, as shown, and also for the $L = \infty$ for the pure T state (not shown), give straight lines, and the intermediate values give curves with downward curvature.

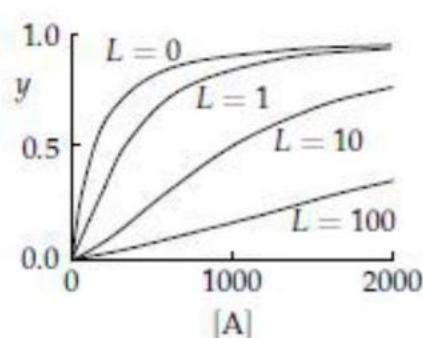


Figure 12.35. Linear scale of concentration. Some of the curves from [Figure 12.34](#) are redrawn with a linear scale of concentrations.

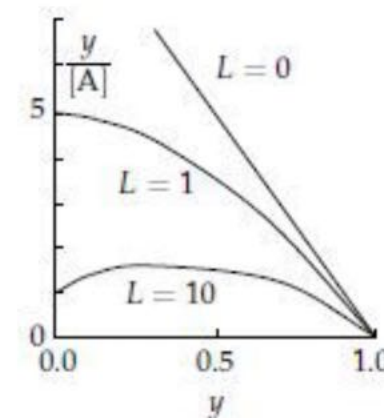


Figure 12.36. Scatchard plots for the symmetry model. Some of the curves from [Figure 12.34](#) are redrawn as Scatchard plots.

12.5.4 Heterotropic effects

Monod and co-workers distinguished between *homotropic effects*, or interactions between identical ligands, and *heterotropic effects*, or interactions between different ligands, such as a substrate and an allosteric effector. Although the symmetry model requires homotropic effects to be positively cooperative, it places no corresponding restriction on heterotropic effects, and it can accommodate these with no extra complications; this is, indeed, one of its most satisfying features. If a second ligand B binds preferentially to the R state of the protein, the state preferred by A, at a different site from A (so that there is no competition between them), it facilitates binding of A by increasing the availability of molecules in the R state; it thus acts as a positive heterotropic effector, or allosteric activator. On the other hand, a ligand C that binds preferentially to the T state, which binds A weakly or not at all, has the opposite effect: it hinders the binding of A by decreasing the availability of molecules in the R state, and will thus act as a negative heterotropic effector, or allosteric inhibitor. If all binding is *exclusive*, which means that each ligand binds either to the R state or to the T state, but not to both, the resulting binding equation for A, as modified by the presence of B and C, is particularly simple, as the allosteric constant L can now be replaced by an apparent value L^{app} that increases with the inhibitor concentration and decreases with the activator concentration, reflecting the capacity of inhibitors to displace the equilibrium away from the state that favors substrate binding, and of activators to displace it towards the same state:

$$y = \frac{\left(1 + \frac{[A]}{K_R}\right) \frac{[A]}{K_R}}{L^{\text{app}} + \left(1 + \frac{[A]}{K_R}\right)^2} = \frac{\left(1 + \frac{[A]}{K_R}\right) \frac{[A]}{K_R}}{L \left(\frac{1 + \frac{[C]}{K_{CT}}}{1 + \frac{[B]}{K_{BR}}} \right)^2 + \left(1 + \frac{[A]}{K_R}\right)^2}$$

When ligands do not bind exclusively to one or other state, the behavior is naturally more complicated, but one can still get a reasonable idea of the possibilities by examining [Figure 12.34](#) in the light of [equation 12.21](#).

High concentrations of allosteric effectors of either sort clearly tend to decrease the cooperativity, as they make the protein resemble either pure R or pure T, but there may be effects in the opposite direction at low concentrations if the value of L (the value of L^{app} in the absence of effectors) is not optimal. In [Figure 12.34](#), for example, the steepest curve occurs with $L = 100$, and that for $L = 10$ is less steep: any concentration of activator tends to decrease L^{app} , taking it further from $L^{\text{app}} = 100$, and hence making it less cooperative.

However, adding an allosteric inhibitor initially increases the cooperativity, to a maximum at $L^{\text{app}} = 100$, but further increases in inhibitor concentration tend to decrease it. If the value of L were greater than 100 rather than less, it would be the activator that would increase the cooperativity at low concentrations, whereas the inhibitor would decrease the cooperativity at all concentrations. These tendencies are not entirely obvious from examination of the curves in [Figure 12.34](#), because in the middle of the range the differences in steepness are not immediately apparent to the eye. However, one can get a correct impression of the directions in which the steepness changes from the fact that the curves at the extremes are noticeably less steep than the one in the middle.

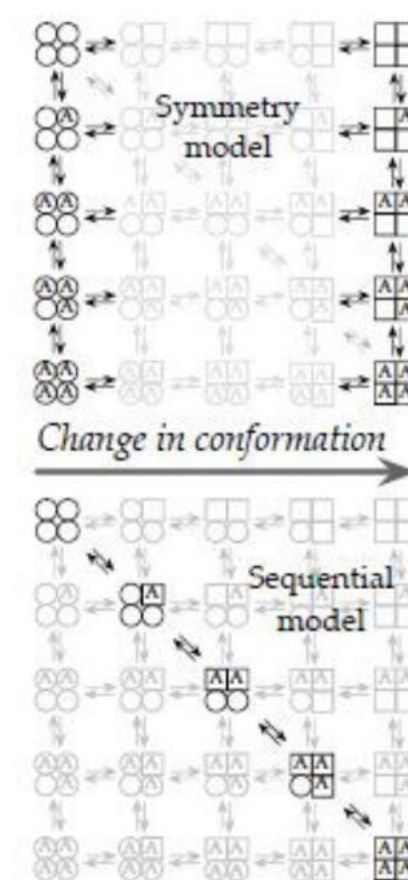


[Figure 12.37](#). Comparison between the simplest forms of the principal models of cooperativity.

A complication arises if we consider an ordinary (nonallosteric) competitive inhibitor that binds to the R state at exactly the same sites as the substrate A. This is considered in Problem 12.5 at the end of this chapter. The binding properties of phosphofructokinase from *Escherichia coli* were thoroughly studied by Blangy and co-workers: over a wide range of concentrations of ADP and phosphoenolpyruvate, an allosteric activator and inhibitor respectively, the binding of the substrate fructose 6-phosphate proved to agree well with the predictions of the symmetry model. Nonetheless, it cannot be regarded as a universal explanation of binding cooperativity, because it cannot explain the negative cooperativity observed for some enzymes, and some of its postulates are not altogether convincing. The central assumption of conformational symmetry is not readily explainable in structural terms, for example, and for many enzymes it is necessary to postulate the occurrence of a “perfect K system”, which means that the R and T states of the enzyme have identical catalytic properties despite having grossly different binding properties. These and other questionable aspects of the symmetry model have stimulated the search for alternatives.

12.6 Comparison between the principal models of cooperativity

The other major model of cooperativity is the *sequential model* of Koshland and co-workers, which we shall consider formally in the next section. First, however, it will be useful to pause to compare it with the symmetry model just discussed. Both assume that cooperativity arises from interactions between subunits in an oligomeric protein, and thus neither can explain how a monomeric protein might exhibit cooperativity ([Section 12.9](#)), and both assume that the interactions result from the possibility of each subunit to exist in more than one conformation. However, the symmetry model treats the different conformations as existing independently of ligand binding, whereas the sequential model treats changes in conformation as intimately linked to the binding of ligand. Haber and Koshland showed how both models can be regarded as special cases of a general model in which all possible combinations of degree of conformational change and degree of binding can exist. For a tetrameric protein with the four subunits arranged as a square, therefore, one could suppose that 25 different states could exist, as shown in [Figure 12.37](#). However, the symmetry model considers only the ten states in the first and last columns, whereas the sequential model considers only the states along the diagonal.

§ 12.9, pages 320–323

Strictly we should talk of the *simplest* symmetry and sequential models,¹⁸ because the proponents of both models have at times considered variants in which some of the postulates are relaxed. However, even the simplest versions make predictions that are often difficult to distinguish experimentally, and very little is gained by making them more complicated than necessary. Over the years since these models were proposed, many authors have proposed general models of which they are special cases. However, although this is obviously possible, as [Figure 12.37](#) shows, it is not obviously useful, except as a purely qualitative exercise.

12.7 The sequential model of Koshland, Némethy and Filmer

12.7.1 Postulates

Although the symmetry model incorporates the idea of purposive conformational flexibility, it departs from the theory of induced fit in permitting ligands to bind to both R and T conformations, albeit with different binding constants. Koshland and co-workers showed that a more orthodox application of induced fit, known as the *sequential model*, could account for cooperativity equally well. Like Monod and co-workers, they postulated the existence of two conformations, which they termed the A and B conformations, corresponding to the T and R conformations respectively.¹⁹ This inversion of the order in which they are usually spoken has sometimes been a source of confusion, and for that reason, and also to allow continued use of A as a symbol for substrate, as elsewhere in this book, the symbols T and R will be used here²⁰. In contrast with the symmetry model, Koshland and co-workers assumed that the R conformation was induced by ligand binding, so that substrate binds only to the R conformation, the R conformation exists only with substrate bound to it, and the T conformation exists only with substrate not bound to it.

Koshland and co-workers postulated that cooperativity arose because the properties of each subunit were modified by the conformational states of the neighboring subunits. The same assumption is implicit in the symmetry model, but it is emphasized in the sequential model, which is more concerned with the details of interaction, and avoids the arbitrary assumption that all subunits must exist simultaneously in the same conformation. Hence conformational hybrids, such as TR in a dimer, or T_3R , T_2R_2 and TR_3 in a tetramer, are not merely allowed, but follow directly from the assumption of strict induced fit.

Because the symmetry model was not concerned with the details of subunit interactions, there was no need in [Section 12.5](#) to consider the geometry of subunit association, the quaternary structure of the protein. By contrast, the sequential model does require consideration of geometry, for any protein with more than two subunits, because different arrangements

of subunits result in different binding equations. Here we shall consider a dimer for simplicity (Figure 12.38), and the geometry can then be ignored, but it cannot be ignored when extending the treatment to trimers, tetramers and so on.

The emphasis on geometry and the need to treat each geometry separately have given rise to the widespread but erroneous idea that the sequential model is more general and complicated than the symmetry model, but for any given geometry the two models are about equally complicated and neither is a special case of the other. As illustrated in Figure 12.37 above, they can both be generalized into the same general model, by relaxing the symmetry requirement of the symmetry model and the strict induced-fit requirement of the sequential model.

§ 12.5, pages 304–312

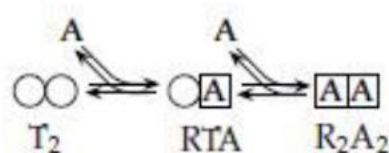


Figure 12.38. Sequential model for a dimeric protein.

To see how a binding equation is built up in the sequential model, consider the changes that occur when a molecule T_2 binds one molecule of A to become RTA, as illustrated in detail in Figure 12.39:

1. There is a statistical factor of 2, because there are two equivalent ways of choosing one out of two subunits to bind A. (The word “equivalent” is essential here, because nonequivalent choices would lead to distinguishable molecules that would have to be treated separately.)
2. The T:T interface is lost when we consider a T subunit in isolation. We include no equilibrium constant for this, for the reasons given in paragraph 5 below.
3. One subunit must undergo the conformational change $T \rightarrow R$, a change represented by the notional equilibrium constant $K_t = [T]/[R]$ for an isolated subunit. In the simplest version of the sequential model K_t is tacitly assumed to be large, so that the change occurs to a negligible extent if it is not induced by ligand binding.
4. One molecule of A binds to a subunit in the R conformation, represented by $[A]/K_A$, where K_A is the intrinsic dissociation

constant $[R][A]/[RA]$ for binding of A to an isolated subunit in the R conformation.

5. In a dimer there is one interface across which the two subunits can interact. In the initial T_2 molecule these are evidently two T subunits, so it is a T:T interface, but in RTA it becomes a T:R interface, a change represented by a notional equilibrium constant $K_{R:T} = [R:T]/[T:T]$. Notice that this definition means that the stability of the T:R interface is defined in terms of a *change* from the T:T interface as not as an absolute measure. That is why no equilibrium constant was introduced in step 2 to represent the loss of the T:T interface. In the original discussion by Koshland and co-workers there was some confusion about whether subunit interaction terms should be regarded as absolute measures of interface stability (logically requiring an additional constant $K_{T:T}$), or whether they should be regarded as measures of the stability relative to a standard state (the T:T interface). The latter interpretation is just as rigorous, simpler to apply (because it leads to constants that are inherently dimensionless, so there is no question of ignoring dimensions), and leads to simpler equations with fewer constants; it will be used here.

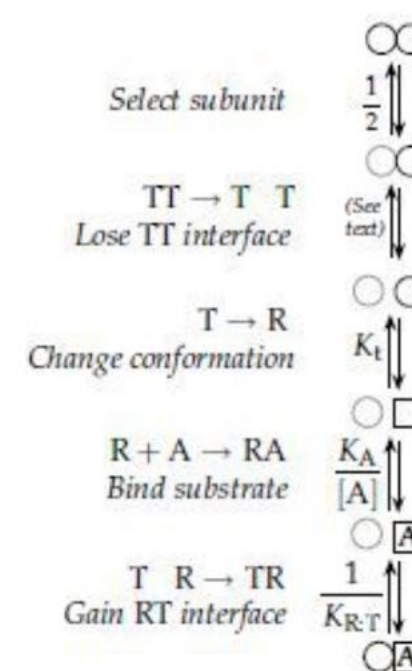


Figure 12.39. Steps in conversion of T_2 to RTA. Descriptions are expressed in the forward direction, but the equilibrium constants are defined in the direction of dissociation.

12.7.2 Algebraic analysis

Putting all this together we may write down the following expression for the concentration of RTA in terms of those of T_2 and A:

$$[RTA] = \frac{2[T_2][A]K_{R:T}}{K_t K_A} \quad (12.22)$$

Although using a dimer as an example allows the sequential model to be explained with minimal complications, it leaves one or two essential aspects of the model unexplained, so we must pause briefly to consider what expression would result from applying the same rules to the formation of a molecule $R_2T_2A_2$ from a tetramer T_4 . We cannot now ignore geometry, because there are at least three different possible arrangements. Here we shall suppose that they interact as if arranged at the corners of a square, and that of the two different ways in which two ligand molecules can be bound to such a molecule (Figure 12.40) we are dealing with the one in which the two ligand molecules are on adjacent (rather than diagonal) subunits. This gives a concentration of

$$[R_2T_2A_2]_{\text{adjacent}} = \frac{4[T_4][A]^2 K_{R:T}^2 K_{R:R}}{K_t^2 K_A^2} \quad (12.23)$$

As there is now a new kind of interface between the two adjacent subunits in the R conformation with ligand bound, we need a new kind of subunit interaction constant, $K_{R:R}$, which, like $K_{T:R}$, is defined relative to the T:T interface, but otherwise equation 12.23 is constructed in just the same way as equation 12.22, from the same components. A tetrahedral geometry, as in Figure 12.41, requires a different analysis.

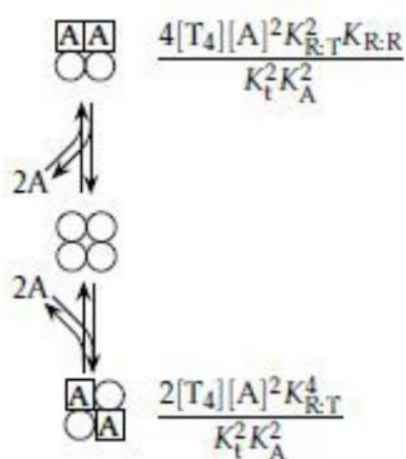


Figure 12.40. Square interaction. If the subunits interact as if arranged in a square there are two different $R_2T_2A_2$ molecules according to whether the occupied subunits are adjacent or diagonal, which must be analyzed separately. Note that the statistical factors are different in the two cases.

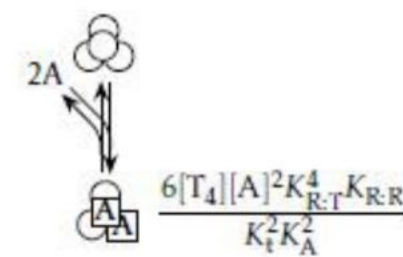


Figure 12.41. Tetrahedral interaction. If the subunits interact as if arranged in a tetrahedron there is just one kind of $R_2T_2A_2$ molecule.

Returning now to the dimer, we can write down an expression for the concentration of R_2A_2 according to the same principles:

$$[R_2A_2] = \frac{[T_2][A]^2 K_{R:R}}{K_t^2 K_A^2} \quad (12.24)$$

Substituting equations 12.22 and 12.24 into the expression for the fractional saturation, we have:

$$y = \frac{[RTA] + 2[R_2A_2]}{2([T_2] + [RTA] + [R_2A_2])} = \frac{\frac{[A]K_{R:T}}{K_t K_A} + \frac{[A]^2 K_{R:R}}{K_t^2 K_A^2}}{1 + \frac{2[A]K_{R:T}}{K_t K_A} + \frac{[A]^2 K_{R:R}}{K_t^2 K_A^2}} \quad (12.25)$$

The sequential model is closely concerned with subunit interactions, and the essential question that an equation such as equation 12.25 answers is how binding of a ligand is affected by the stability of the mixed interface R:T relative to mean stability of the interfaces R:R and T:T between subunits in like conformations. Inspection of equation 12.25 shows that making $K_{R:T}$ smaller increases the importance of the outer terms with respect to the inner, but this can be made clearer by defining a constant $c^2 = K_{R:T}^2 / K_{R:R}$ to express this relative stability. (It may seem surprising at first sight that there is no mention of the T:T interface in this definition, but remember that both $K_{R:T}$ and $K_{R:R}$ already define the stabilities of the R:T and R:R interfaces relative to the T:T interface.)

If $K_{R:T}$ is replaced by $c K_{R:R}^{1/2}$, using this definition, it then becomes clear that $\bar{K} = K_t K_A / K_{R:R}^{1/2}$ always occurs as a unit: its three components are conceptually distinct, but they cannot be separated experimentally by means of binding measurements. The equation can thus be simplified in appearance without loss of generality by writing it in terms of c and \bar{K} :

$$y = \frac{\frac{c[A]}{K} + \frac{[A]^2}{K^2}}{1 + \frac{2c[A]}{K} + \frac{[A]^2}{K^2}} \quad (12.26)$$

$$\frac{v}{V} = \frac{\frac{a}{K_1} + \frac{a^2}{K_1 K_2}}{1 + \frac{2a}{K_1} + \frac{a^2}{K_1 K_2}} \quad (12.5)$$

The definition of c is the same for all quaternary structures: it applies not only to dimers, but also to trimers, tetramers, and so on, regardless of how the subunits are arranged. The definition of K is a little more complicated: it always contains $K_t K_A$ as an inseparable unit (as follows from steps 1 and 2 in the description above of how any binding process is decomposed into different notional components); on the other hand, the power to which $K_{R:R}$ is raised in the denominator varies with the number of subunits and with the number of R:R interfaces that the fully liganded molecule contains. However, this has little importance: the important point is that regardless of quaternary structure and geometry the range of binding behavior possible for a single ligand in the sequential model is determined by two parameters, one to represent the stability of the R:T interface with respect to the R:R and T:T interface, the other an average dissociation constant for the complete binding process from fully unliganded to fully liganded protein. This is the geometric mean²¹ of the Adair dissociation constants, as may be seen for the dimer by writing these explicitly, after comparing [equation 12.26](#) with [equation 12.5](#) (repeated above in the margin):

$$K_1 = \frac{K}{c}; \quad K_2 = cK \quad (12.27)$$

with ratio $K_2/K_1 = c^2$.

12.7.3 Properties implied by the binding equation

It is now clear that the degree of cooperativity, and hence the shape of the binding curve, depends only on the value of c . As illustrated in [Figure 12.42](#), values of $c < 1$ generate positive cooperativity and values of $c > 1$ generate negative cooperativity. The effect of varying K is not shown (to avoid

making the figure too complicated), but can be stated simply: it has no effect on the shapes of the curves when $\ln[A]$ is the abscissa (and affects only the scaling with other variables as abscissa), but simply causes them to be shifted to the right (if K increases) or left (if K decreases); in other words, K has no effect on the degree of cooperativity. The curve for $c = 10$ is doubly sigmoid, with a noticeable decrease in slope around half-saturation. This effect becomes more pronounced with larger values of c and leads to *half-of-the-sites reactivity*

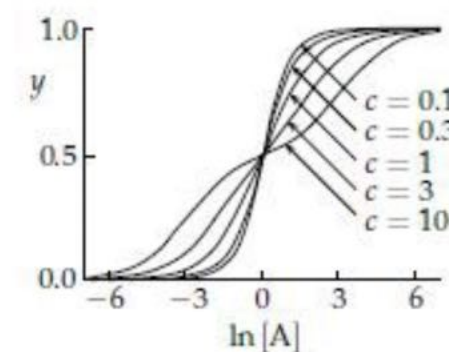


[Figure 12.42](#). Binding curves for the sequential model. The curves are calculated from [equation 12.26](#), with $K = 1000$ and the values of c shown. The value of K does not affect the shape of a curve, but only its location along the abscissa.

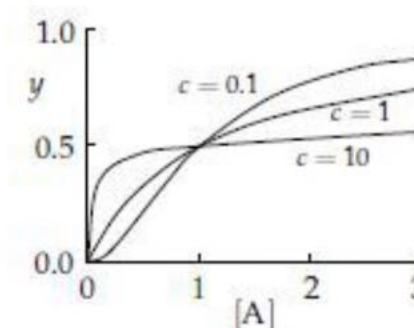


[Figure 12.43](#). Binding curves with a linear scale of concentration. Some of the curves of [Figure 12.42](#) are rescaled.

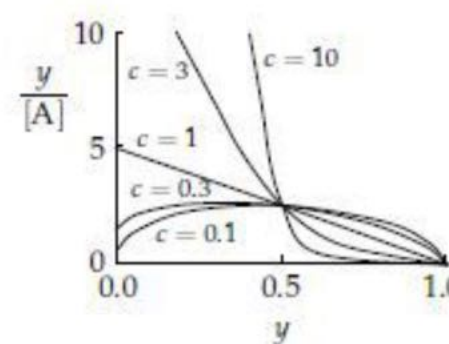


[Figure 12.44](#). Scatchard plots for the sequential model. The curves of [Figure 12.42](#) are redrawn.

The cooperative case generates a visibly sigmoid curve when a linear scale is used for the ligand concentration ([Figure 12.43](#)), but the negatively cooperative curve is qualitatively similar to the noncooperative curve. As with the symmetry model, the

degree of deviation from linearity is very evident in Scatchard plots ([Figure 12.44](#)).

It would be convenient if there were a simple correspondence between the parameters of the sequential model and those of the Hill equation ([equation 12.1](#)), but although, as we have seen, the degree of cooperativity depends only on c , there is no one-to-one relationship between h and c , as h varies with the degree of saturation and c does not. By contrast, the relationship between K and $K_{0.5}$, the half-saturation concentration, is as simple as one could ask: they are identical.

As incorrect statements are sometimes found in the literature one should notice that in the sequential model the shape of the curve is defined by fewer parameters than in the symmetry model (one instead of two). Thus the capacity of the sequential model to explain negative cooperativity whereas the symmetry model cannot is not a consequence of the large number of constants considered in deriving the sequential model (K_t , K_A , $K_{R:T}$ and $K_{R:R}$).

More subtle misconceptions about the sequential model are implied by some authors' use of names such as "Adair–Koshland model" or "Pauling–Koshland model" for it. Although crediting it to Adair, as done, for example, by Wimpenny and Moroz, correctly implies that the sequential model is a special case of the Adair model it also incorrectly implies that the symmetry model is not. In reality, both models are expressible in terms of Adair constants ([equations 12.19](#) and [12.27](#)), as, indeed, any valid equation to describe binding of a ligand to a macromolecule at equilibrium must be. The simplest test of meaningfulness that one can apply to a proposed equation written for this purpose is adherence to the Adair equation; equations that are not special cases of the Adair equation, such as some that Weber and Anderson proposed for lactate dehydrogenase, generally violate the principle of microscopic reversibility ([Section 5.6](#)).²²

Likewise, some of the mathematics in the sequential model is the same as that applied by Pauling to hemoglobin, but the underlying concepts are different: he was working at a time when it was reasonable to suppose that the oxygen-binding sites of hemoglobin were close enough together in space to interact in an ordinary chemical way, and there was no implication of conformational interactions.

For a positively cooperative dimer there is no difference between the binding curves that the two models can predict: any value less than 1 of the ratio K_2 / K_1 of Adair constants that one can give is consistent with the other. It is thus impossible to distinguish between them on the basis of binding experiments with a dimer. In principle they become different for trimers and higher oligomers, because the symmetry model then allows the binding curves plotted as a function of $\ln [A]$ (as in [Figure 12.34](#)) to become unsymmetrical about the half-saturation point, whereas the corresponding curves generated by the sequential model (as in [Figure 12.42](#)) are always symmetrical with respect to rotation through 180° about this point. However, the departures from symmetry are quite small, and highly accurate data are needed to detect them. Moreover, the greatest degree of cooperativity occurs in the symmetry model when $Lc^n = 1$, and as this is also the condition for a symmetrical binding curve in the symmetry model one may expect that for at least some enzymes evolution will have eliminated any asymmetry that might have existed.

12.8 Association-dissociation models of cooperativity

Various groups (Frieden; Nichol and co-workers) independently suggested that cooperativity might in some circumstances result from the existence of an equilibrium between protein forms in different states of aggregation, such as a monomer and a tetramer. If a ligand has different intrinsic dissociation constants for the two forms, then this model predicts cooperativity even if there is no interaction between the binding sites in the tetramer. Conceptually the model is rather similar to the symmetry model, and the cooperativity arises in a similar way, but the equations are more complicated, because they need to take account of the dependence of the degree of association on the protein concentration. Consequently, in contrast to the equations for the symmetry and sequential models, this concentration does not cancel from the expressions for the saturation curves. This type of model is much more amenable to experimental verification than the other models we have considered, because the effects of protein concentration ought to be easily observable. They have indeed

been observed for a number of enzymes, such as glutamate dehydrogenase (Frieden and Colman) and glyceraldehyde 3-phosphate dehydrogenase (Ovádi and co-workers), and other examples were noted by Kurganov, who discussed association–dissociation models in detail.

12.9 Kinetic cooperativity

All the models discussed in the earlier part of this chapter have been essentially equilibrium models that can be applied to kinetic experiments only by assuming that v/V is a true measure of y . Cooperativity can also arise for purely kinetic reasons, in mechanisms that would show no cooperativity if binding could be measured at equilibrium. This was known from the studies of Ferdinand and of Rabin and others when the classic models of cooperativity were being developed, but at that time there did not seem to be experimental examples of cooperativity in monomeric enzymes. As a result it was widely assumed that even if multiple binding sites were not strictly necessary for generating cooperativity they provided the only mechanisms actually found in nature, and the purely kinetic models were given little attention. However, rat-liver hexokinase D provided an example of positive cooperativity in a monomeric enzyme, making it clear that models for such properties would need to be considered seriously.

Hexokinase D is an enzyme found in the liver and pancreatic islets of vertebrates. Because of a mistaken perception that it is more specific for glucose than the other vertebrate hexokinases, discussed by Cárdenas and co-workers, it is frequently known in the literature as “glucokinase”, but this name will not be used here. It is monomeric over a wide range of conditions, including those used in its assay (Holroyde and co-workers; Cárdenas and co-workers), but it shows marked deviations from Michaelis–Menten kinetics when the glucose concentration is varied at constant concentrations of the other substrate, MgATP^{2-} (Niemeyer and co-workers; Storer and Cornish-Bowden). When replotted as Hill plots, the data show h values ranging from 1.5 at saturating MgATP^{2-} to a low value, possibly 1.0, at vanishingly small MgATP^{2-} concentrations. On the other hand, it shows no deviations from Michaelis–Menten kinetics with respect to MgATP^{2-} itself.

Other examples of cooperativity in monomeric enzymes are not abundant, but they exist (see Cornish-Bowden and Cardenas), and indicate that mechanisms that generate kinetic cooperativity can no longer be ignored. I shall consider two such mechanisms in this section. The older is due to Ferdinand, who pointed out that the steady-state rate equation for the random-order ternary-complex mechanism ([Section 8.3.2](#)) is much more complicated than [equation 8.7](#) if it is derived without assuming substrate-binding steps to be at equilibrium; he suggested that a model of this kind, which he called a *preferred-order mechanism*, might provide an explanation for the cooperativity of phosphofructokinase. It is clear enough from consideration of the method of King and Altman ([Chapter 5](#)) that deviations from Michaelis–Menten kinetics ought to occur with this mechanism, but this explanation is rather abstract and algebraic. In conceptual terms the point is that both pathways for substrate binding may make significant contributions to the total flux through the reaction, but the relative magnitudes of these contributions change as the substrate concentrations change. Thus the observed behavior corresponds approximately to one pathway at low concentrations, but to the other at high concentrations.

Ricard and co-workers developed an alternative model of kinetic cooperativity from earlier ideas of Rabin and Whitehead. Their model is known as a *mnemonical* model (from the Greek for memory),²³ because it depends on the idea that the enzyme changes conformation relatively slowly, and is thus able to “remember” the conformation that it had during a recent catalytic cycle. It is shown (in a simplified form) in [Figure 12.45a](#). It postulates that there two forms E and E' of the free enzyme differ in their affinities for A, the first substrate to bind; in addition equilibration between E, E', A and EA must be slow relative to the maximum flux through the reaction. With these postulates, the behavior of hexokinase D is readily explained. As the concentration of B is lowered, the rate at which EA is converted into EAB and thence into products must eventually become slow enough for E, E', A and EA to equilibrate. At vanishingly small concentrations of B, therefore, the binding of A should behave like an ordinary equilibrium, with no cooperativity, because there is only a single binding site. At high concentrations

of B, on the other hand, it becomes possible for EA to be removed so fast that it cannot equilibrate and the laws of equilibria no longer apply (Storer and Cornish-Bowden). Deviations from Michaelis–Menten kinetics are then possible because at low concentrations of A the two forms of free enzyme can equilibrate (Figure 12.45b), favoring E', but at high concentrations they cannot (Figure 12.45c), leaving the free enzyme predominantly in the form E released after the chemical reaction.

§ 8.4.1, pages 204–207

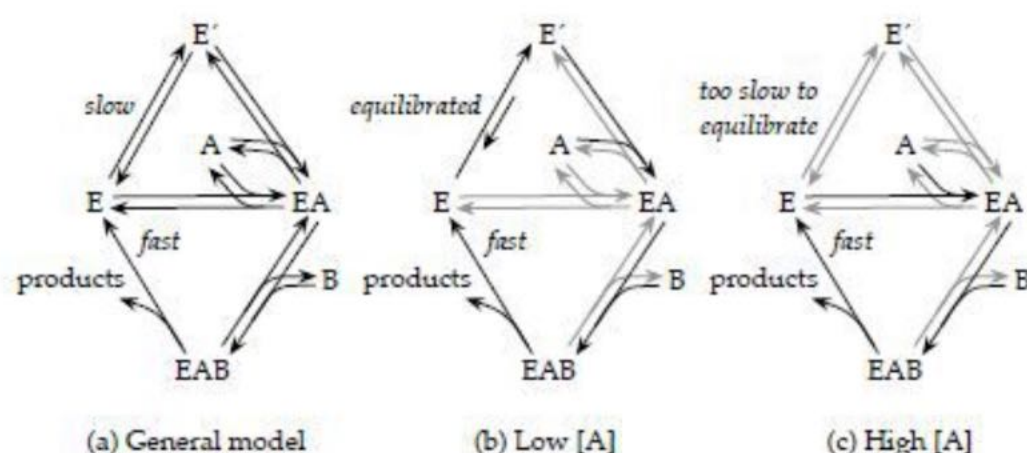


Figure 12.45. Mnemonical model. (a) General characteristics. (b) At low concentrations of A. Even if the second substrate B is at a high enough concentration to remove EA as soon as it is formed, binding of A to the free enzyme is slow enough for E and E' to equilibrate. (c) At high concentrations of it can bind to the high-affinity form E before it has time to decay to E'

In the mnemonical mechanism as proposed for wheat-germ hexokinase by Ricard and co-workers the same form of EA complex is produced from both forms of free enzyme when substrate binds to them. However, this is not a necessary feature of the model, and the *slow-transition model* developed a little earlier by Ainslie and co-workers supposes that two different conformational states exist during the whole catalytic cycle, with transitions between them possible at any point that occur at rates that are slow compared with the catalytic rate. In general, any model that allows substrate to bind in two or more parallel steps will generate a rate equation with terms in the square or higher power of the concentration of the substrate concerned, so there is no limit to the models of kinetic cooperativity that can be devised. Unfortunately it is quite difficult in practice to distinguish between them or to assert with much confidence that one fits the facts better than another. Certainly, both the mnemonical and slow-transition

models are able to explain the behavior of hexokinase D adequately, as Cárdenas discusses thoroughly in her book. The existence for multiple conformation in the hexokinase D reaction was originally deduced from kinetic considerations, but there is now abundant evidence, for example from nuclear magnetic resonance studies by Larion and co-workers, that the conformational changes are real and large, as illustrated above in Figure 12.30.

Summary of Chapter 12

- *Michaelis–Menten kinetics allow very little sensitivity to changes in conditions, and so effective regulation of metabolism requires certain enzymes, known as **regulatory enzymes**, to follow more complicated kinetics.*
- **Cooperativity** is the property whereby an enzyme can have a steep dependence on substrate or inhibitor concentration.
- **Allosteric effects** allow regulation by molecules that do not bind at the same sites as the substrates and products.
- The **Hill equation** is useful for expressing the degree of cooperativity in quantitative terms, but it is not based on a realistic mechanism.
- The **symmetry model** of Monod, Wyman and Changeux explains cooperativity in terms of an oligomeric protein with all subunits in the same conformation at any time.
- The **sequential model** of Koshland, Némethy and Filmer explains cooperativity in terms of interactions between the subunits of an oligomeric protein.
- **Association-dissociation models** of cooperativity explain it in terms of effects of ligands on the state of oligomerization of a protein.
- Kinetic cooperativity can arise in a **monomeric enzyme** from slow relaxations between different conformational states.

§ 12.1, pages 281–286

§ 12.1.3, page 284

§ 12.1.4, pages 285–286

§§ 12.2.1–12.2.2, pages 286–288

§§ 12.5–12.6, pages 304–312

§§ 12.6–12.7, pages 312–319

§ 12.8, pages 319–320